[CANCER RESEARCH 61, 1548–1554, February 15, 2001]

Targeting a Genetically Engineered Elastin-like Polypeptide to Solid Tumors by Local Hyperthermia[1]

Dan E. Meyer, Garheng A. Kong, Mark W. Dewhirst, Michael R. Zalutsky, and Ashutosh Chilkoti[2]

Department of Biomedical Engineering, Duke University, Durham, North Carolina 27708 [D. E. M., G. A. K., A. C.], and Departments of Radiation Oncology [M. W. D.] and Radiology [M. R. Z.], Duke University Medical Center, Durham, North Carolina 27710

ABSTRACT

Elastin-like polypeptides (ELPs) are biopolymers of the pentapeptide repeat Val-Pro-Gly-Xaa-Gly that undergo an inverse temperature phase transition. They are soluble in aqueous solutions below their transition temperature (T_t) but hydrophobically collapse and aggregate at temperatures greater than T_t. We hypothesized that ELPs conjugated to drugs would enable thermally targeted drug delivery to solid tumors if their T_t were between body temperature and the temperature in a locally heated region. To test this hypothesis, we synthesized a thermally responsive ELP with a T_t of 41°C and a thermally unresponsive control ELP in *Escherichia coli* using recombinant DNA techniques. *In vivo* fluorescence videomicroscopy and radiolabel distribution studies of ELP delivery to human tumors (SKOV-3 ovarian carcinoma and D-54MG glioma) implanted in nude mice demonstrated that hyperthermic targeting of the thermally responsive ELP for 1 h provides a ~2-fold increase in tumor localization compared to the same polypeptide without hyperthermia. We observed aggregates of the thermally responsive ELP by fluorescence videomicroscopy within the heated tumor microvasculature but not in control experiments, which demonstrates that the phase transition of the thermally responsive ELP carrier can be engineered to occur *in vivo* at a specified temperature. By exploiting the phase transition-induced aggregation of these polypeptides, this method provides a new way to thermally target polymer-drug conjugates to solid tumors.

INTRODUCTION

The delivery of drugs to solid tumors remains a critical problem in the treatment of cancer. Achieving therapeutic drug levels within a tumor is impeded by transport barriers due to the complex physiology and morphology of the tumor. Furthermore, chemo- and radiotherapeutic agents are typically toxic to healthy cells in addition to tumor cells, and undesirable side effects are common in anticancer therapy. In an attempt to overcome these problems, different types of drug delivery systems have been developed that use macromolecules, vesicles, or particles as carriers for therapeutics (1–5). In general, these systems seek to optimize whole-body pharmacokinetics and to maximize localization of the drug to the tumor (1).

Soluble macromolecular carriers are useful drug delivery vehicles because they increase the plasma half-life of low molecular weight drugs, increase the solubility of hydrophobic drugs, provide passive targeting to tumors by the enhanced permeability and retention effect (6), and can also permit controlled release of the drug through the use of degradable linkers (5). Because vascular permeability increases at temperatures between 40°C and 45°C, hyperthermia treatments can also enhance the delivery of drugs to solid tumors (7). Furthermore, when combined with chemo- and radiotherapy, hyperthermia can synergistically enhance tumor cytotoxicity (8, 9).

Here, we propose a novel thermal targeting scheme using a thermally responsive, genetically engineered ELP.[3] ELPs are biopolymers of the pentapeptide repeat Val-Pro-Gly-Xaa-Gly, where the "guest residue" Xaa can be any of the natural amino acids except Pro (10). ELPs undergo an inverse temperature phase transition; they are soluble in aqueous solutions below their T_t, but they hydrophobically collapse and aggregate at temperatures greater than T_t (10, 11). We hypothesized that an ELP with a T_t intermediate between T_b and T_h would enable thermally targeted drug delivery to a locally heated region. In this scenario, the ELP would be soluble systemically because its inverse T_t ($T_t \approx 41$°C) is greater than T_b ($T_b \approx 37$°C–38°C), but it would become insoluble and accumulate in locally heated regions where the temperature was increased above T_t by externally targeted hyperthermia ($T_h \approx 42$°C–43°C). In concept, this method synergistically combines thermal targeting through the ELP phase transition with the established advantages of both polymeric carriers (*e.g.*, increased plasma half-life, high loading capacity) and hyperthermia as an anticancer treatment modality (*e.g.*, increased sensitivity to therapeutics, greater macromolecular tumor extravasation).

MATERIALS AND METHODS

ELP Design. The T_ts of the ELPs were controlled at the polypeptide sequence level by specifying the fraction and identity of the fourth, guest residue in the pentapeptide repeat. A thermally responsive ELP termed ELP1 was designed to have a target T_t of 41°C by incorporation of Val, Gly, and Ala in a 5:3:2 ratio, respectively, at the guest residue position of the pentapeptide. We also designed a thermally unresponsive control ELP (ELP2) with physicochemical properties similar to those of ELP1 (*e.g.*, composition and molecular weight) but with a predicted T_t well above T_h (>55°C) so that it would not undergo its phase transition in heated tumors. The control ELP2 had guest residues Val:Gly:Ala in the ratio of 1:7:8. The guest residue ratios were selected for ELP1 and ELP2 based on the previous results of Urry *et al.* (12), who characterized the relationship between T_t and guest residue identity and mole fraction.

ELP Synthesis. Our approach to the synthesis of ELPs has been described elsewhere (13). Briefly, synthetic genes encoding the two different ELP sequences were constructed as follows (Fig. 1). Short gene segments (10 pentapeptides for ELP1 and 16 pentapeptides for ELP2) were assembled by annealing chemically synthesized oligonucleotides (Integrated DNA Technologies, Coralville, IA) encoding the sense and antisense strands to form a gene cassette, which was then ligated into pUC19 (New England Biolabs, Beverly, MA). These DNA segments were oligomerized by a process we term "recursive directional ligation," a convenient and flexible method to rapidly assemble a specified number of tandem gene repeats in a defined orientation.[4] The final gene encoded 150 ELP pentapeptides for ELP1 and 160 pentapeptides for ELP2. The oligomerized genes were then excised from pUC19 and ligated into a modified pET25b expression vector (Novagen, Madison, WI). The expression vector contained translation initiation and termination codons and the codons for short leading (Ser-Lys-Gly-Pro-Gly) and trailing (Trp-Pro) sequences. Standard molecular biology protocols were used for all DNA manipulations (14).

Received 10/30/00; accepted 1/3/01.

The costs of publication of this article were defrayed in part by the payment of page charges. This article must therefore be hereby marked *advertisement* in accordance with 18 U.S.C. Section 1734 solely to indicate this fact.

[1] Supported by a grant from the Whitaker Foundation (to A. C.), NIH Grant CA42745 (to M. W. D.), and Department of Energy Grant DE-F602-96ER62148 (to M. R. Z.).

[2] To whom requests for reprints should be addressed, at Department of Biomedical Engineering, Campus Box 90281, Duke University, Durham, NC 27708-0281.

[3] The abbreviations used are: ELP, elastin-like polypeptide; SIB, *N*-succinimidyl 3-iodobenzoate; T_b, physiological body temperature; T_h, temperature in the hyperthermic region; T_t, transition temperature.

[4] D. E. Meyer, and A. Chilkoti. Genetically encoded synthesis of protein-based polymers with precisely specified molecular weight by recursive directional ligation, manuscript in preparation.

ELP1

```
ATG AGC AAA GGG CCG GGC (GTG GGT GTT CCG GGC GTG GGT GTT CCG
 (M)  S   K   G   P   G  (V   G   V   P   G   V   G   V   P
GGT GGC GGT GTG CCG GGC GCA GGT GTT CCT GGT GTA GGT GTG CCG
 G   G   G   V   P   G   A   G   V   P   G   V   G   V   P
GGT GTT GGT GTG CCG GGT GTT GGT GTA CCA GGT GGC GGT GTT CCG
 G   V   G   V   P   G   V   G   V   P   G   G   G   V   P
GGT GCA GGC GTT CCG GGT GGC GGT GTG CCG GGC)15 TGG CCG TGA
 G   A   G   V   P   G   G   G   V   P   G      W   P  (ter)
```

ELP2

```
ATG AGC AAA GGG CCG GGC (GTG GGT GTG CCG GGC GCA GGT GTT CCG
 (M)  S   K   G   P   G  (V   G   V   P   G   A   G   V   P
GGT GGC GGT GTG CCG GGC GCA GGT GTT CCG GGT GGC GGT GTG CCG
 G   G   G   V   P   G   A   G   V   P   G   G   G   V   P
GGC GCA GGT GTT CCG GGT GGC GGT GTG CCG GGC GCA GGT GTT CCG
 G   A   G   V   P   G   G   G   V   P   G   A   G   V   P
GGT GGC GGT GTG CCG GGC GCA GGT GTT CCG GGT GGC GGT GTG CCG
 G   G   G   V   P   G   A   G   V   P   G   G   G   V   P
GGC GCA GGT GTT CCG GGT GGC GGT GTG CCG GGC GCA GGT GTT CCG
 G   A   G   V   P   G   G   G   V   P   G   A   G   V   P
GGT GGC GGT GTG CCG GGC GCA GGT GTG CCG GGC)10 TGG CCG TGA
 G   G   G   V   P   G   A   G   V   P   G      W   P  (ter)
```

Fig. 1. Gene and corresponding polypeptide sequences for ELP1 and ELP2. The genes were synthesized by oligomerization of a gene segment shown in *bold*. The polymerized gene region was flanked by short leading and trailing sequences. The genes were expressed in *E. coli* using the pET25b T7-lac expression vector.

The ELPs were expressed in the *Escherichia coli* strain BLR(DE3) (Novagen). The ELPs were purified from other *E. coli* proteins in the soluble fraction of the cell lysate by inverse transition cycling (13, 15). The ELPs were characterized for purity and molecular weight by SDS-PAGE visualized by copper staining (16). The molecular weights of the polypeptides determined by comparison with a molecular weight standard were consistent with the expected values of M_r 59,400 for ELP1 and M_r 61,100 for ELP2.

Characterization of the Inverse Transition. The inverse temperature phase transition of the ELPs was characterized by monitoring the absorbance at 350 nm as a function of temperature on a UV-visible spectrophotometer equipped with a multicell thermoelectric temperature controller (Cary 300 Bio; Varian Instruments). Reversibility of the transition was examined by first heating an ELP solution in PBS, typically from 20°C to 60°C at a rate of 1°C/min, and then cooling the solution to 20°C at the same rate. The T_t was defined from the heating profile as the temperature at 5% of maximum turbidity.

Labeling. The ELP constructs have two primary amines (the NH_2 terminus and a single lysine at the second residue). Labels for the *in vivo* experiments were conjugated to these amines using succinimidyl ester chemistry. Rhodamine Red-X succinimidyl ester (Molecular Probes, Inc.) was used for the fluorescence videomicroscopy experiments, and SIB (17) was used for the radiolabeling experiments, where the iodine was either ^{131}I, ^{125}I, or ^{127}I (nonradioactive). For paired label biodistribution studies, ELP1 was conjugated to [^{131}I]SIB, and ELP2 was conjugated to [^{125}I]SIB.

In a typical conjugation reaction, ELP1 or ELP2 was dissolved in 100 mM sodium bicarbonate (pH 8.4). The reporter, which was dissolved at a concentration of 10 mg/ml in dimethylformamide, was slowly added while mixing to a final molar excess of ~4 for rhodamine-to-ELP coupling and ~40 for SIB-to-ELP coupling. The reactants were incubated with continuous stirring for 2 h at room temperature. Insoluble matter was removed by centrifugation at 4°C. The ELP was then purified from soluble free label by inverse transition cycling. Labeling yield was calculated using UV-visible spectrophotometry (UV-1601; Shimadzu Scientific Instruments, Inc.). Typically, the molar label: ELP ratio was ~0.5 for rhodamine and ~1.0 for SIB.

Serum Stability. The rhodamine-ELP and SIB-ELP conjugates were separately diluted 1:6 in fresh, heparinized mouse serum. This dilution ratio approximates that of the *in vivo* experiments. The ELP-serum mixture was then incubated at 37°C for up to 2 days, and aliquots were removed for analysis at various times points for analysis by SDS-PAGE, which separated the conjugated and free label into distinct bands. The conjugates were visualized under UV transillumination and quantitated by scanning densitometry. Free and conjugated SIB were separated by instant TLC, and each fraction was counted for radioactivity.

***In Vivo* Fluorescence Videomicroscopy.** Athymic mice were implanted with dorsal skin fold window chambers containing a small piece of tumor tissue (~0.1 mm^3 human ovarian carcinoma; SKOV-3) placed near the center of the window (18–20). The preparations were used 7–8 days after implantation, when the tumors had grown to 2–3 mm in diameter. The mice were anesthetized with sodium pentobarbital (80 mg/kg, i.p.) and positioned laterally recumbent on a microscope stage (Carl Zeiss, Inc., Thornwood, NY). The window chamber, which was connected to a temperature-controlled water bath that had been previously calibrated to the temperature within the chamber (7, 21), was maintained either at the physiological s.c. temperature in mice, 34°C (7), or at 42°C. A region of the tumor containing clearly visible tumor microvasculature was selected under transillumination with a ×20 objective. Then, under epi-illumination using a dichroic filter set for rhodamine, images were acquired by a SIT camera (Hamamatsu C2400-08) and recorded in S-VHS format (Mitsubishi BV-1000). In a typical experiment, 200 μl of 100 μM rhodamine-labeled ELP in PBS (~1.2 mg/mouse) were injected into the cannulated tail vein. Three groups of five animals each were studied: (*a*) ELP1 at 42°C; (*b*) ELP2 at 42°C; and (*c*) ELP1 at 34°C. Images were recorded continuously for 40 s after injection and for 10 s every 2 min for 50 min.

Image Analysis of *in Vivo* Fluorescence Videomicroscopy. Accumulation of the rhodamine-labeled ELPs in the tumors was quantified by digital analysis of the videomicrographs as follows. A TIFF image was created for each of 33 time points (10 s preinjection; 30 s, 1 min, and 2 min after injection; and every 2 min thereafter up to 50 min) by averaging 30 frames over 3 s of footage using Scion Image v. 1.62 (NIH Image, as modified by Scion Corp.). The images were analyzed for total window fluorescence intensity and for fluorescence intensity subdivided in the vascular and interstitial spaces within the total window. For total window intensity, the average pixel value was calculated for the entire window (440 × 515 μm). The background (the 10 s preinjection time point) was subtracted from each of the other time points, which were then normalized to the initial time point (30 s after injection). For calculating the relative vascular and interstitial intensities, regions in the 30 s postinjection videomicrograph were defined as either vascular or interstitial. These definitions were determined by numerically computing the gradient of the intensity at each point (*i.e.*, pixel) in the window and then using a threshold parameter to define the edges of vessels. The average intensity of these edges was calculated for subregions of the image. Pixels within the subregion that had an intensity greater than the local average for the edges and the edges themselves were classified as vascular. These spatial definitions were then used as a mask for later time points, allowing pixel values to be averaged independently for the interstitial and vascular regions. The average intensities for the vascular and interstitial areas were analyzed by subtracting the background and normalizing the initial vascular average intensity.

Tumor Localization Studies. Athymic mice (Balb/C *nu/nu*) were inoculated s.c. on the lateral thigh with 50 μl of tumor homogenate (human glioma; D-54MG). The experiments were performed 7–10 days later, when the tumors had grown to at least 3 mm in diameter. The mice were anesthetized with sodium pentobarbital (80 mg/kg, i.p.), and the tumor-bearing leg was taped into a wire jig that allowed each mouse to be suspended such that only the leg was immersed in a temperature-controlled water bath maintained at 43.7°C (22). There were two groups of five animals each; one group received the hyperthermia treatment, whereas the other, normothermic control group was left at room temperature. At the beginning of the experiment, [^{125}I]SIB-ELP1 and [^{131}I]SIB-ELP2 (3 μCi of each) were coinjected into the tail vein of each mouse. The radiolabeled ELPs were supplemented with ELPs conjugated to nonradioactive SIB so that the total dose injected was ~300 μg of each ELP per animal (each ELP at 50 μM in 100 μl of PBS). After 45 min, both groups were euthanized with an overdose of halothane (Halocarbon Laboratories, River Edge, NJ). The tumors were resected and counted for radioactivity on a LKB 1282 dual-channel gamma counter (Wallac), with crossover correction for ^{131}I spillover into the ^{125}I counting window.

RESULTS AND DISCUSSION

Design and Synthesis of ELPs. The thermally responsive ELP1 was designed to have a T_t of ~41°C. This T_t was chosen because it is greater than the normal body temperature but lower than temperatures that can be readily achieved clinically by focused hyperthermia methods (23). We hypothesized that ELP1 would be systemically soluble below T_t, but would become insoluble and aggregate in the target region where the temperature was greater than T_t. We controlled the T_t by adjusting the hydrophobicity of the amino acid sequence (12). For ELP1, the T_t was increased to 41°C from 27°C, which is the T_t of the natural elastin repeat VPGVG (12), by substi-

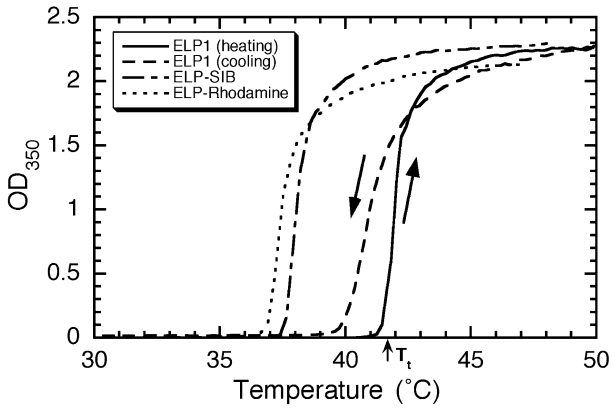

Fig. 2. Turbidity (OD_{350}) as a function of temperature for unlabeled ELP1 and for its SIB and rhodamine conjugates. The turbidity profiles of the polypeptides (25 μM in PBS) were obtained at a rate of 1°C/min. Heating and cooling traces (marked by *arrows*) for unlabeled ELP1 show that the transition is completely reversible. The inverse transition of the rhodamine and SIB conjugates is also reversible; however, for clarity, only the heating profiles are shown. Conjugation of the labels lowered the T_t by ~5°C compared with free ELP.

tuting Ala and Gly for the more hydrophobic Val at the fourth position of the pentapeptide. The thermally unresponsive control, ELP2, was designed to have a T_t greater than T_h by incorporating a greater fraction of hydrophilic Ala and Gly residues so that it would remain soluble even in the heated tissues.

***In Vitro* Characterization of ELPs.** The inverse transition behaviors of both ELP1 and ELP2 were characterized by monitoring solution turbidity as a function of temperature. Fig. 2 shows a heating and cooling turbidity profile for the ELP1 carrier. Below the T_t, the polypeptide solution was clear, but upon further heating, the solution became turbid because of ELP aggregation. The rapid increase in turbidity upon reaching T_t shows that the transition is very sharp with respect to temperature, occurring over a range of less than 2°C. The inverse transition of each ELP was completely reversible, and no end point hysteresis was observed. The slight difference between the paths of the heating and cooling traces is due to the slower kinetics of disaggregation as compared with aggregation. From the heating turbidity profiles, the T_t is defined as the temperature at the onset of turbidity (5% maximal turbidity) to precisely characterize the first appearance of ELP aggregates.

Fig. 2 also shows that conjugation of SIB and rhodamine reduced the ELP1 T_t by ~4°C. We hypothesize that this shift is caused by hydrophobic interactions facilitated by the close proximity of the conjugated, nonpolar labels and the ELP chain, analogous to the decrease in the T_t observed with increasing guest residue hydrophobicity. Loss of the hydrophilic, charged amine groups on conjugation may similarly contribute to the T_t reduction. The decrease in T_t after conjugation has important implications for the loading of ELPs as therapeutic carriers, particularly for drugs with a significant hydrophobic character. The decrease of T_t by ~4°C observed here does not require any compensation other than an adjustment of the ELP plasma concentration during thermally targeted delivery (discussed below). However, for drugs that are more hydrophobic or for higher drug: carrier loading ratios, the carrier can be designed to have a higher T_t in anticipation of a larger downward shift caused by conjugation of the drug.

We also studied the effect of mixing ELP1 and ELP2 on their inverse transition behaviors. This has direct relevance to the tumor biodistribution studies carried out with ELP1 and ELP2, which were conjugated to [^{131}I]SIB and [^{125}I]SIB, respectively, mixed in equimolar proportions, and injected. Coinjected paired labels are desirable because they enable the simultaneous study of the tumor localization of both the thermally responsive (ELP1) and thermally unresponsive (ELP2) carriers in the same animal, thereby minimizing the effect of animal-to-animal physiological variability. To use paired labels, however, it was critical to understand whether ELP1 and ELP2 in mixture would each exhibit independent aggregation at their respective T_ts or whether they would display a cooperative transition behavior that would preclude paired label biodistribution studies using coinjected ELP1 and ELP2.

The inverse transition behavior of an equimolar ELP1 and ELP2 was monitored by a solution turbidity assay in PBS supplemented with 1 M NaCl (Fig. 3). (1 M NaCl was added to depress the T_t so that the transitions of both components in the mixture could be observed in an experimentally convenient temperature range.) The mixture showed biphasic aggregation behavior: on increasing the temperature, two distinct aggregation events were observed that closely overlaid the aggregation profiles for ELP1 and ELP2 obtained separately. We conclude that the T_ts for ELP1 and ELP2 are sufficiently different such that interactions between the more hydrophilic ELP2 and the relatively hydrophobic ELP1 are minimal, even after ELP1 has undergone its transition to the collapsed state. These results clearly show that ELP1 and ELP2 maintain independent aggregation behavior in solution, indicating that paired label studies can be used with these carriers.

Cosolutes, including salts and soluble plasma proteins, also alter the T_t of ELPs (11, 13). We simulated the *in vivo* environment by measuring the T_t in PBS with 0.9 mM BSA, which was added to mimic the effect of plasma proteins. A BSA concentration of 0.9 mM was chosen empirically through a pilot experiment in which the ELP1 T_t was determined in freshly collected, heparinized mouse plasma and compared with its T_t in PBS as a function of BSA concentration (Fig. 4). PBS with 0.9 mM BSA and murine plasma both reduced the ELP1 T_t by ~4°C compared with distilled water.

ELP concentration is also known to affect the T_t (24). Fig. 5 shows that the T_t is an inverse logarithmic function of ELP concentration. Therefore, although serum cosolutes and the conjugation of hydrophobic reporters and drugs act to *decrease* the T_t for a given concentration, the *increase* in T_t with decreasing concentration can be exploited to compensate for these effects. Achieving and maintaining the intended ELP plasma concentration are important considerations for thermal targeting because if the *in vivo* concentration is too high, the T_t will drop below T_b, and the carrier will undergo its phase transition systemically. This would eliminate selective targeting to the heated region and could potentially deliver an unintended dose of aggregated carrier to other organs. Conversely, if the *in vivo* concentration is too

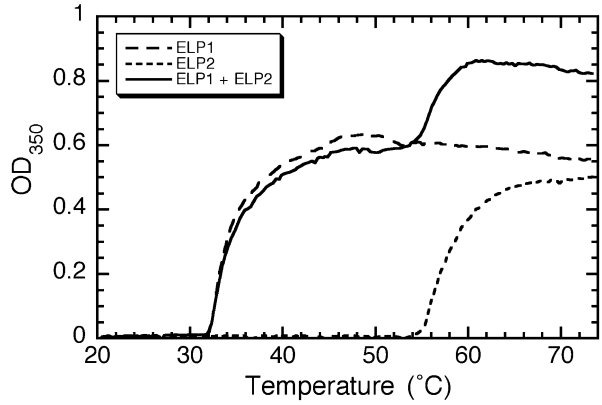

Fig. 3. Effect of mixing ELP1 and ELP2 on their inverse transition behavior in PBS supplemented with 1 M NaCl. In a mixture of ELP1 (1 μM) and ELP2 (1 μM), each ELP underwent its transition independently, similar to that seen in separate 1 μM solutions.

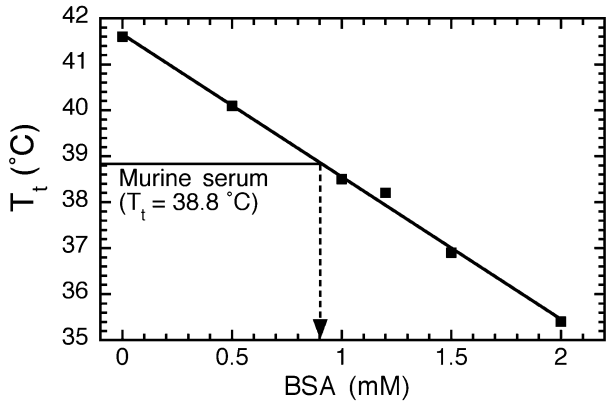

Fig. 4. T_t (defined as the temperature at 5% maximal turbidity) of ELP1 in PBS as a function of added BSA. An independent measurement of the inverse transition behavior of ELP1 in mouse serum showed that the effect of serum on the inverse transition could be approximated by 0.9 mM BSA in PBS.

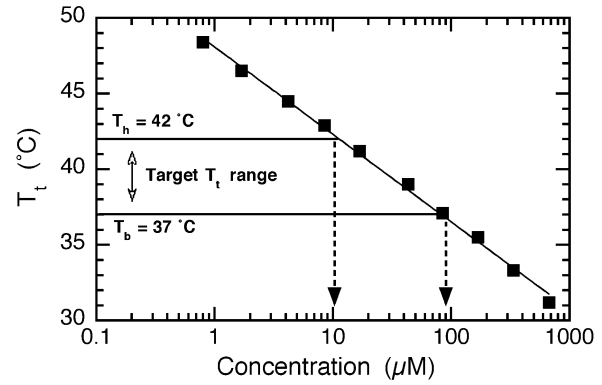

Fig. 5. T_t as a function of ELP1 concentration, showing an inverse logarithmic relationship (*solid line*). To estimate the *in vivo* T_t, the experiments were performed in PBS supplemented with 0.9 mM BSA. The ELP dose is selected to result in a desired target T_t of ~41°C *in vivo* after dilution in plasma.

low, then the T_t would be greater than T_h, and the carrier will remain soluble systemically. Although this would eliminate thermal targeting to the heated tumor, this latter outcome is less problematic because there would also be no thermally induced aggregation in nontargeted organs. During therapy, T_t should therefore remain above T_b but can safely be allowed to increase to above T_h (*e.g.*, as the carrier concentration decreases with time due to systemic clearance).

Despite these constraints, the dependence of T_t on ELP concentration does not severely limit the applicability of ELP thermal targeting because the effect is logarithmic, and thus only a relatively small change in T_t is caused by a large change in ELP concentration. With ELP1, for example, a T_t can be achieved in the range that is clinically available for thermal targeting between 37°C and 42°C over a ~10-fold range in ELP concentration (Fig. 5). If higher or lower ELP doses are required for therapy, ELP sequences with different compositions can be readily synthesized such that they exhibit a T_t between 37°C and 42°C in a different range of concentrations as compared with ELP1. We also note that if the total dose of drug needs to be limited below a specified threshold as defined by its systemic toxicity, free ELP carrier can be mixed with the ELP-drug conjugate to provide the necessary polypeptide concentration required to achieve the target T_t.

Based on these results and experimental considerations, we selected a target plasma concentration of 5 μM for the radiolabel *in vivo* experiments. Turbidity profiles of the SIB-labeled ELP1 inverse transition in the PBS + 0.9 mM BSA solution indicated that this ELP concentration will yield in a T_t of 41°C in blood (data not shown). We then calculated the dose required to achieve this concentration using an estimated mouse plasma volume of 1 ml (25–26).

Serum Stability. Before the *in vivo* experiments, we tested the stability of the fluorescent (rhodamine) and radioactive (SIB) conjugates in serum as a function of time. No ELP degradation was observed; however, both labels were cleaved over time. No loss of SIB was observed in ELP incubated in physiological saline (Fig. 6*A*), which suggests that the cleavage was due to an enzyme present in the serum. Fig. 6*A* also shows that the SIB-ELP conjugate was stable over time, and ~90% remained conjugated after 48 h in serum. The rhodamine label was cleaved from the ELP more rapidly, with only 60% remaining conjugated after 24 h (Fig. 6*B*). However, over the 1-h time frame of the *in vivo* experiments, loss of either label from the ELP carrier was negligible (<2%).

***In Vivo* Studies.** Temperature-controlled *in vivo* fluorescence videomicroscopy of ELP-rhodamine conjugate enabled real-time visualization of its accumulation within the tumor. Three different sets of animals were studied ($n = 5$ for each set): (*a*) ELP1 injected with the tumor heated (T_h = 42°C). (*b*) ELP2 injected with heating (T_h = 42°C); and (*c*) ELP1 injected without heating (T_b = 34°C). Image analysis of the total fluorescence intensity in the window allows quantitative comparison between the three groups, provided that the measured fluorescence intensity is linearly related to fluorophore concentration, as has been previously established for our experimental conditions (20). We assume that immediately after injection, the carrier is present only in the vasculature. The data were therefore normalized to the initial fluorescence intensity (30 s after injection) to correct for variations between animals, in the injected dose, and in fluorescence intensity between the ELPs (*i.e.*, due to differences in rhodamine conjugation efficiency).

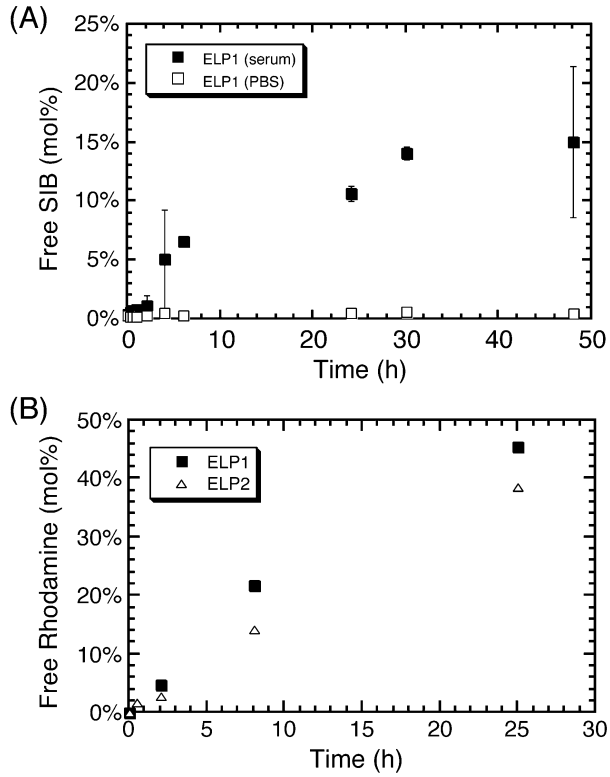

Fig. 6. Stability in murine serum at 37°C as a function of time for SIB and rhodamine conjugated to ELPs. *A*, percentage of free SIB as a function of incubation time for the ELP1-SIB conjugate in serum (■) and in physiological saline (□). *B*, percentage of free rhodamine as a function of incubation time for the ELP-rhodamine conjugates in serum. ■, ELP1; △, ELP2.

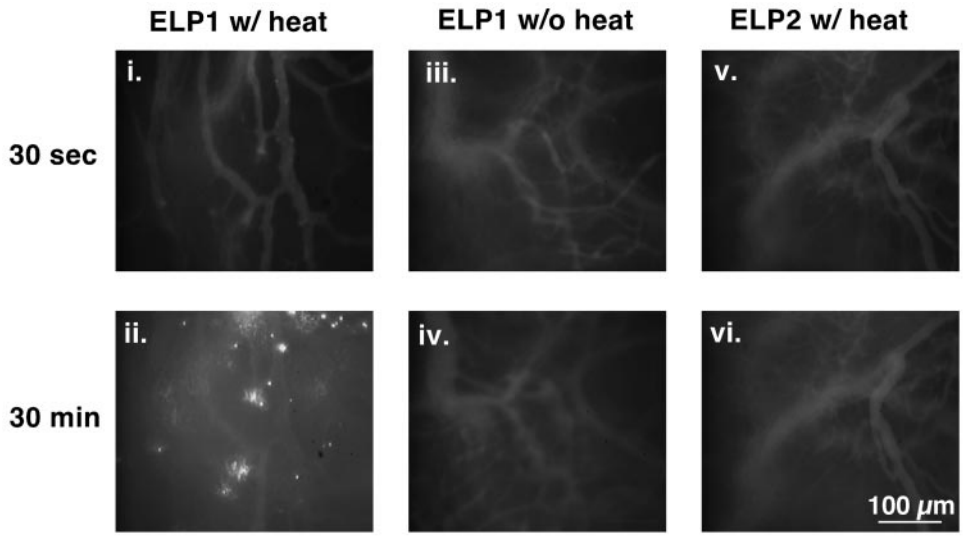

Fig. 7. Window chamber fluorescence videomicrographs of tumor tissue at 30 s and 30 min after injection of the ELPs. The thermally responsive carrier, ELP1, was injected, and the window was maintained at 42°C (*i.* and *ii.*). For the low temperature control group, the same ELP1 carrier was injected, but the window was not heated (*iii.* and *iv.*). For the high temperature control group, the thermally unresponsive carrier, ELP2, was injected, and the window was maintained at 42°C (*v.* and *vi.*). ELP aggregates (*ii.*) were observed only for ELP1 in tumors heated to 42°C and demonstrate that the inverse temperature phase transition occurred *in vivo*. Increased extravasation was also observed for ELP1 with hyperthermia relative to both controls.

Fig. 7 shows representative videomicrographs acquired at 30 s and at 30 min after injection for all three groups of animals. Within 1–2 min after the thermally responsive ELP1 carrier was injected into mice with window chambers heated to 42°C, fluorescent particles were observed (Fig. 7, *ii.*). None were observed for ELP1 without hyperthermia (Fig. 7, *iv.*) or for ELP2 with hyperthermia (Fig. 7, *vi.*) at any time, strongly suggesting that these particles are ELP aggregates resulting from the inverse temperature transition. The aggregates often attached to the vessel wall, and they grew in intensity and size over time. Once attached to the vessel wall, the aggregates were typically stable throughout the experiment. More rarely, as the particles grew larger, they were sheared from the vessel walls and carried away by the blood flow. Because the inverse transition is reversible, any particles washed from the heated tissue would be expected to rapidly disaggregate and resolubilize. The observation of ELP1 aggregates only in the heated window chambers is an exciting finding because, to our knowledge, it is the first *in vivo* demonstration that a thermal phase transition of a free polymer in solution can be engineered to occur at a specified temperature within a complex physiological system.

The relative fluorescence intensities obtained by image analysis of the entire window are summarized in Fig. 8. Over the first 30 min, the accumulation of ELP1 in the heated tumor increased rapidly. For the remainder of the experiment, however, tumor ELP levels remained constant. The reason for this apparent saturation could be systemic clearance or local depletion of the ELP from the circulation. Decreasing plasma ELP concentration could have caused the T_t to increase above T_h, as described above, thereby halting any further accumulation. After 50 min, the total window intensity had increased 250% relative to the initial window intensity at 30 s. This represents a nearly 70% greater tumor accumulation of ELP1 in the heated tumor as compared with ELP1 at 34°C and a 54% increase *versus* ELP2 at 42°C. For all time points after 4 min, ELP1 delivery to the heated tumor was significantly greater than that for both the unheated ELP1 ($P < 0.05$) and heated ELP2 ($P < 0.1$) control groups.

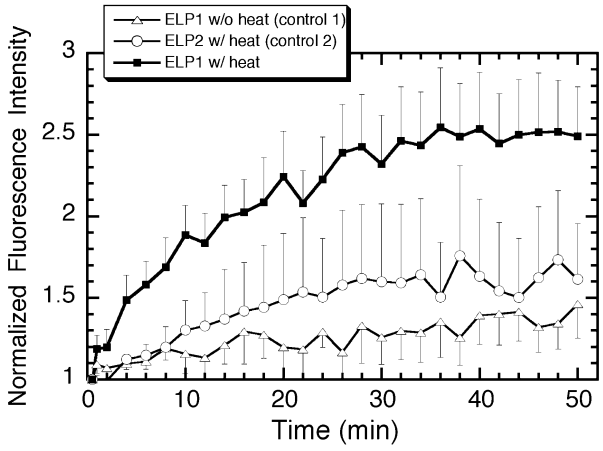

Fig. 8. Total window fluorescence intensity of tumor as a function of time after injection of ELP-rhodamine conjugate, background corrected and normalized to the initial intensity at 30 s postinjection (mean ± SE; $n = 5$). ELP1 without heat, △; ELP2 with heat, ○; ELP1 with heat, ■. For times greater than 4 min, the fluorescence intensity of ELP1 with heat was significantly greater than that of unheated ELP1 ($P < 0.05$, unpaired *t* test) and heated ELP2 ($P < 0.1$, unpaired Mann-Whitney test).

We also examined the spatial distribution of the ELPs within the tumor microstructure. A masking algorithm was developed to enable regions in the window chamber videomicrographs to be explicitly defined as either vascular or interstitial. These spatial definitions were then applied as a mask throughout the remainder of the experiment to determine the average fluorescence intensity in each region, enabling the vascular and interstitial ELP concentrations to be tracked directly as a function of time. We note that this analysis is semiquantitative in that cross-over between the two regions is inherent in this analysis. Scatter in the interstitium of fluorescent light emitted from the blood vessels is detected as having originated in the interstitium, and light emitted from the interstitium above and below a vessel is detected as having originated in the vessel. Despite this, the analysis nonetheless provides useful insight into the dynamic, albeit relative, partitioning of the carrier within the tumor as a function of experimental conditions.

Fig. 9 shows the interstitial and vascular fluorescence intensities quantitated using this algorithm for ELP1 in the heated tumor. At the initial 30 s time point, the interstitial intensity was measured as 53% of the vasculature. Both regions increased in intensity over the course of the experiment, although the interstitium increased more rapidly, and, at 50 min, its intensity had increased to 86% of the vasculature. Accumulation in the interstitial space is likely due to extravasation of both soluble ELP and small aggregates, presumably via endothelial cell gaps, and is perhaps enhanced by further aggregation once extravasated. Thus, these results suggest that in addition to the larger aggregates that accumulate in the vessels, extravasation of the ELP also plays an important role in the total ELP accumulation observed

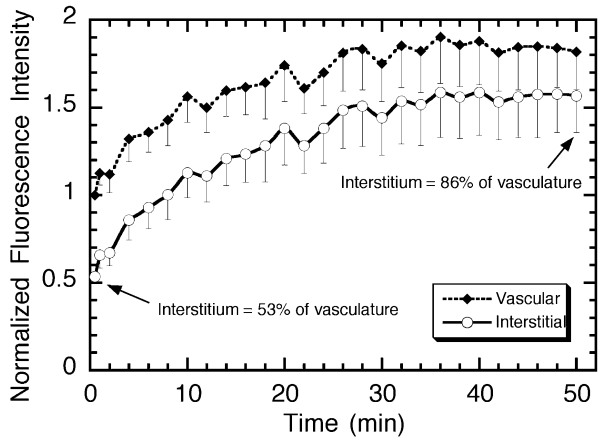

Fig. 9. Fluorescence intensity of vasculature (♦) and interstitium (○) in the window chamber as a function of time after injection of ELP1-rhodamine conjugate in the heated tumor (mean ± SE; $n = 5$). Accumulation of ELP1 increased through the course of the experiment for both regions, although the interstitial intensity grew more rapidly, suggesting that increased extravasation is an important factor leading to tumor localization.

within the heated tumor. Studies on the mechanism via which the ELPs interact with endothelial and tumor cells as a function of temperature are currently in progress to elucidate the origin of this effect.

We also independently studied thermal targeting of the ELP carrier by directly determining the localization of radiolabeled ELP in implanted tumors, with and without hyperthermia. Fig. 10 shows that tumor localization of the thermally responsive ELP1 was 80% greater for the animals that received the hyperthermia treatment than for the same ELP in unheated tumors ($P < 0.01$). Unlike the window chamber experiment, the data for the high temperature control were obtained from the same animals using coinjected, paired radiolabels. For animals treated with hyperthermia, tumor accumulation of ELP1 (with $T_b < T_t < T_h$) was 34% greater than that for ELP2 (for which $T_t > T_h$; $P < 0.005$). From the combined data of the two controls, we conclude that ~60% of the total increase in ELP1 tumor accumulation *versus* the nonheated group can be attributed to the effects of the ELP inverse transition, and ~40% is contributed by the physiological effects of hyperthermia. It is notable that the percentage increase in tumor accumulation of the heated, thermally responsive carrier *versus* both controls in the radiolabel distribution experiments is consistent with the results from the quantitative analysis of the window chamber experiments. Finally, there was no significant difference in tumor localization between ELP1 and ELP2 for the unheated control group, indicating that the thermally responsive and unresponsive carriers behaved similarly in the absence of heat. This demonstrates that ELP2, with its composition and molecular weight virtually identical to those of ELP1, is a well-designed, thermally unresponsive control.

The controls for the experiments described here were carefully designed to elucidate the separate effects of changes in tumor physiology due to hyperthermia and of the thermally triggered phase transition of the ELP on localization of the carrier in solid tumors. These controls should also prove useful in future optimization studies seeking to maximize the effect of the phase transition on tumor accumulation of the carrier. However, it is critical that the results of the current study be viewed in the context of drug delivery using macromolecular carriers. The observed ~2-fold increase in ELP1 accumulation in heated tumors is *not* relative to free drug. Soluble macromolecular carriers can provide up to several orders of magnitude greater delivery and specificity (*e.g.*, passive tumor targeting due to the enhanced permeability and retention effect) to the tumor *versus* free drug (1, 6), particularly for low molecular weight drugs with rapid renal clearance and for hydrophobic drugs with low solubility. Therefore, the increase in tumor delivery due to the ELP inverse temperature transition should be viewed as a synergistic factor that further amplifies the advantages of using macromolecular carriers to deliver drugs to solid tumors.

Although other thermally responsive drug carriers such as temperature-sensitive liposomes and cross-linked hydrogels have been proposed (27–29), to our knowledge, this is the first reported use of a thermally responsive polymer as a soluble carrier for thermal drug targeting. One advantage of this system over other thermally responsive carriers is that accumulation of the drug in the target tissue is driven through a phase transition of the carrier rather than through thermally triggered release of the drug. A concentration gradient is therefore not required to drive accumulation of the ELP, which will continue to accumulate through phase separation in a heated tumor (provided that $T_t < T_h$) even when their blood concentration is less than the concentration in the tumor. This is an attractive feature because it enables the ELP-drug conjugate to be injected at a lower and therefore less toxic systemic concentration while still achieving a higher therapeutic concentration in the tumor.

Thermal targeting achieves regional targeting and is not specific to a particular cell type; therefore, any organ or tissue can be targeted independent of the availability of specific ligands or antibodies. For the delivery of radiotherapeutics, regional targeting (*i.e.*, targeting to the tumor as opposed to tumor cells) is sufficient for therapy, and our initial work is therefore focused on their delivery to solid tumors. However, the delivery of other molecules such as chemotherapeutics, oligonucleotides, or imaging agents may require tumor cell-specific targeting. For these applications, thermal targeting could be synergistically combined with a cell-specific affinity-targeting moiety by gene level fusion or chemical conjugation of the targeting moiety (30–32). Alternatively, the ELP could serve as a first stage, systemic targeting method to rapidly increase concentrations in the targeted region. This would be followed by release of the drug through labile linkers, which could also incorporate a secondary, affinity-targeting molecule.

The results presented here should be viewed as preliminary because no attempt has yet been made to optimize important experimental variables. In future studies, the ELP molecular weight is likely to be the most important design criterion to be explored because it is the primary design parameter that controls both plasma half-life and extravasation. The systemic concentration of the drug-ELP conjugate

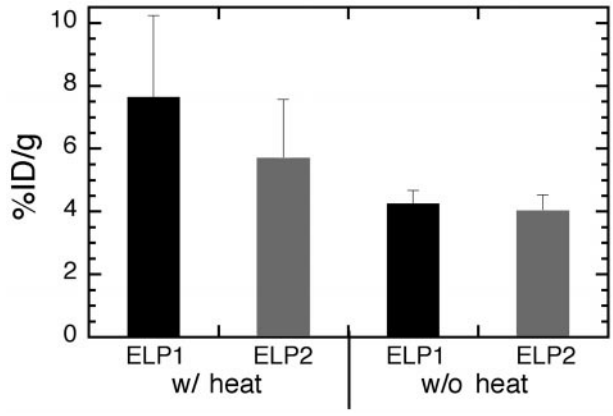

Fig. 10. Tumor localization of radiolabeled ELP (mean ± SE; $n = 5$), expressed as a percentage of the injected dose per gram of tissue. Tumor localization was significantly greater for the thermally responsive carrier (ELP1) when the tumor was heated to 42°C than for the same carrier in the low temperature controls ($P < 0.01$, unpaired, nonparametric Mann-Whitney test). Within the heated group, the thermally responsive ELP accumulated to a significantly greater level as compared with the thermally unresponsive control (ELP2; $P < 0.005$, paired t test). There was no significant difference between ELP1 and ELP2 within the low temperature control group.

is a second important variable because of its effect on T_t, as described above, and because absolute systemic concentration may affect the relative distribution to the heated tumor *versus* other tissues. The administration protocol is the third variable that is likely to have a significant effect on the accumulation of thermally responsive ELPs in heated tumors. Controlled infusion, *versus* a bolus protocol as described in this study, may allow better control over the time course *in vivo* concentration to maintain the T_t in the requisite range ($T_b < T_t < T_h$), thereby ensuring continual carrier accumulation in the tumor throughout the duration of the hyperthermia treatment. Furthermore, initial doses trapped in the hyperthermic region may trap later doses with higher efficiency. This may eventually allow a treatment protocol in which free ELP is initially injected, followed by a lower dose ELP conjugated to a therapeutic agent, thereby maximizing tumor-specific delivery of the therapeutic agent while minimizing systemic toxicity.

In summary, the results presented here demonstrate that a genetically engineered, thermally responsive ELP in combination with hyperthermia exhibits a ~2-fold increase in accumulation in heated tumors compared with the same polypeptide without hyperthermia. Comparison of these results with the accumulation of a thermally unresponsive, control polypeptide revealed that much of the increased accumulation of the thermally responsive polypeptide in heated tumors was caused by the inverse transition and subsequent aggregation of the thermally responsive polypeptide rather than by the nonspecific, physiological effects of hyperthermia. The window chamber studies also revealed that the preferential accumulation of the thermally responsive polypeptide in heated tumors is due to the combined effect of increased accumulation in the vasculature and increased extravasation of the polypeptide within the tumor. The results of this study are notable because they demonstrate, for the first time to our knowledge, the concept of thermal targeting through the exploitation of a soluble-to-insoluble polymeric phase transition that has been designed to occur at a specific temperature *in vivo*. We believe that even greater accumulation of the thermally responsive carrier in tumors may well be achieved after optimization of the this thermal targeting system. Finally, synergistic thermal and affinity targeting schemes offer the tantalizing possibility of further improving the targeted delivery of therapeutics to solid tumors using these thermally responsive polypeptides as macromolecular carriers.

ACKNOWLEDGMENTS

We thank Dr. Catherine Foulon for performing the ELP radiolabeling, Dr. Marlene Hauck and Susan Slade for assistance with the tumor distribution experiments, and Dr. Darell Bigner for providing the D-54MG xenograft mice. We also thank the Whitaker Foundation for support of D. E. M. as a graduate fellow.

REFERENCES

1. Duncan, R. Drug-polymer conjugates: potential for improved chemotherapy. Anticancer Drugs, *3:* 175–210, 1992.
2. Jones, M., and Leroux, J. Polymeric micelles: a new generation of colloidal drug carriers. Eur. J. Pharm. Biopharm., *48:* 101–111, 1999.
3. Torchilin, V. P. Polymer-coated long-circulating microparticulate pharmaceuticals. J. Microencapsul., *15:* 1–19, 1998.
4. Allen, T. M. Liposomal drug formulations: rationale for development and what we can expect in the future. Drugs, *56:* 747–756, 1998.
5. Langer, R. Drug delivery and targeting. Nature (Lond.), *392* (Suppl.)*:* 5–10, 1998.
6. Matsumura, Y., and Maeda, H. A new concept for macromolecular therapeutics in cancer chemotherapy: mechanisms of tumoritropic accumulation of protein and the antitumor agent SMANCS. Cancer Res., *46:* 6387–6392, 1986.
7. Dewhirst, M. W., Prosnitz, L., Thrall, D., Prescott, D., Clegg, S., Charles, C., MacFall, J., Rosner, G., Samulski, T., Gillette, E., and LaRue, S. Hyperthermic treatment of malignant diseases: current status and a view toward the future. Semin. Oncol., *24:* 616–625, 1997.
8. Feyerabend, T., Steeves, R., Wiedemann, G. J., Richter, E., and Robins, H. I. Rationale and clinical status of local hyperthermia, radiation, and chemotherapy in locally advanced malignancies. Anticancer Res., *17:* 2895–2897, 1997.
9. Issels, R. Hyperthermia combined with chemotherapy: biological rationale, clinical application, and treatment results. Onkologie, *22:* 374–381, 1999.
10. Urry, D. W. Free energy transduction in polypeptides and proteins based on inverse temperature transitions. Prog. Biophys. Mol. Biol., *57:* 23–57, 1992.
11. Urry, D. W. Physical chemistry of biological free energy transduction as demonstrated by elastic protein-based polymers. J. Phys. Chem. B, *101:* 11007–11028, 1997.
12. Urry, D. W., Luan, C. H., Parker, T. M., Gowda, D. C., Prasad, K. U., Reid, M. C., and Safavy, A. Temperature of polypeptide inverse temperature transition depends on mean residue hydrophobicity. J. Am. Chem. Soc., *113:* 4346–4348, 1991.
13. Meyer, D. E., and Chilkoti, A. Purification of recombinant proteins by fusion with thermally responsive polypeptides. Nat. Biotechnol., *17:* 1112–1115, 1999.
14. Ausubel, F. M., Brent, R., Kingston, R. E., Moore, D. H., Seidman, J. G., Smith, J. A., and Struhl, K. Current Protocols in Molecular Biology. New York: John Wiley & Sons, 1995.
15. McPherson, D. T., Xu, J., and Urry, D. W. Product purification by reversible phase transition following *Escherichia coli* expression of genes encoding up to 251 repeats of the elastomeric pentapeptide GVGVP. Protein Expression Purif., *7:* 51–57, 1996.
16. Lee, C., Levin, A., and Branton, D. Copper staining: a five-minute protein stain for sodium dodecyl sulfate-polyacrylamide gels. Anal. Biochem., *166:* 308–312, 1987.
17. Zalutsky, M. R., and Narula, A. S. A method for the radiohalogenation of proteins resulting in decreased thyroid uptake of radioiodine. Appl. Radiat. Isot., *38:* 1051–1055, 1987.
18. Dewhirst, M. W., Tso, C. Y., Oliver, R., Gustafson, C. S., Secomb, T. W., and Gross, J. F. Morphologic and hemodynamic comparison of tumor and healing normal tissue microvasculature. Int. J. Radiat. Oncol. Biol. Phys., *17:* 91–99, 1989.
19. Wu, N. Z., Da, D., Rudoll, T. L., Needham, D., Whorton, A. R., and Dewhirst, M. W. Increased microvascular permeability contributes to preferential accumulation of stealth liposomes in tumor tissue. Cancer Res., *53:* 3765–3770, 1993.
20. Wu, N. Z., Klitzman, B., Rosner, G., Needham, D., and Dewhirst, M. W. Measurement of material extravasation in microvascular networks using fluorescence videomicroscopy. Microvasc. Res., *46:* 231–253, 1993.
21. Gross, J. F., Roemer, R., Dewhirst, M. W., and Meyer, M. A uniform thermal field in a hyperthermia chamber for microvascular studies. Int. J. Heat Mass Transfer, *25:* 1313–1320, 1982.
22. Hauck, M. L., Dewhirst, M. W., Bigner, D. D., and Zalutsky, M. R. Local hyperthermia improves uptake of a chimeric monoclonal antibody in a subcutaneous xenograft model. Clin. Cancer Res., *3:* 63–70, 1997.
23. Dewhirst, M. W. Thermal dosimetry. *In:* M. H. Seegenschmiedt, P. Fessenden, and C. C. Vernon (eds.), Principles and Practice of Thermoradiotherapy and Thermochemotherapy, Vol. I, pp. 123–136. Berlin: Springer-Verlag, 1995.
24. Urry, D. W., Trapane, T. L., and Prasad, K. U. Phase-structure transitions of the elastin polypentapeptide-water system within the framework of composition-temperature studies. Biopolymers, *24:* 2345–2356, 1985.
25. Barbee, R. W., Perry, B. D., Re, R. N., and Murgo, J. P. Microsphere and dilution techniques for the determination of blood flows and volumes in conscious mice. Am. J. Physiol., *263:* R728–R733, 1992.
26. Durbin, P. W., Jeung, N., Kullgren, B., and Clemons, G. K. Gross composition and plasma and extracellular water volumes of tissues of a reference mouse. Health Phys., *63:* 427–442, 1992.
27. Kong, G., and Dewhirst, M. W. Hyperthermia and liposomes. Int. J. Hyperth., *15:* 345–370, 1999.
28. Galaev, I. Y., and Mattiasson, B. "Smart" polymers and what they could do in biotechnology and medicine. Trends Biotechnol., *17:* 335–339, 1999.
29. Yuk, S. H., and Bae, Y. H. Phase-transition polymers for drug delivery. Crit. Rev. Ther. Drug Carrier Syst., *16:* 385–423, 1999.
30. Panchagnula, R., and Dey, C. S. Monoclonal antibodies in drug targeting. J. Clin. Pharm. Ther., *22:* 7–19, 1997.
31. Arap, W., Pasqualini, R., and Ruoslahti, E. Cancer treatment by targeted drug delivery to tumor vasculature in a mouse model. Science (Washington DC), *279:* 377–380, 1998.
32. Lu, Z. R., Kopeckova, P., and Kopecek, J. Polymerizable Fab′ antibody fragments for targeting of anticancer drugs. Nat. Biotechnol., *17:* 1101–1104, 1999.